Vol:8, Issue:2
Deccember,2021

International Journal of Electronics and Applied Research (IJEAR)

Design and measurement of S-Band Coaxial to Hexagonal waveguide adapter

J.K. Prajapati , Praful Irpache, and S.S. kakatkar *

AMS Division, Society for Applied Microwave Electronics Engineering and Research (SAMEER) IIT Campus, Powai, Mumbai 400076, INDIA

Abstract

In this paper, the design and measured results for coaxial to hexagonal waveguide adapter have been presented. The method can be extended for other bands as well. Optimization of probe length, diameter of wire used and location of the shorting wall has been done for an S band coaxial to hexagonal waveguide adapter and simulated and measured results demonstrating good agreement with each other have been presented.

1 Introduction

The transition between waveguides to coaxial is a very important and often required component in the measurement of waveguides [Holzman, 2005]. A variety of methods exist for transitions between rectangular waveguide to coaxial for various bands but not much literature is available on the transition between a coaxial to hexagonal waveguide. Hexagonal waveguides are often used for circular polarizers [Bhardwaj and Volakis, 2018] and in polarisation agile wideband phased array antennas [Vaish and Parthasarathy, 2010]. An array of open ended hexagonal waveguides may be used for phased array applications because of their superior packing density due to their shape, as compared to rectangular or circular waveguides [Fang et al., 2019]. Hexagonal waveguide fed slot array can also be used in load bearing phased arrays where the hexagonal waveguide itself becomes one of the masts supporting a structure e.g. on ships or wings of an aircraft or drone [Chen and Vaughan, 2019]. These waveguides can also be used for high power heating and drying applications and can be used for power combining [Bhattacharya and Maity, 2021]. Hence the coaxial to hexagonal waveguide adapter needs to be explored.
In this paper, coaxial to waveguide transitions have been simulated, optimized and designed. The design and experimental setup have been explained in Section 2, whereas the simulated and measured results have been presented Section 3. It has been shown that the simulated and measured results are in good agreement.

*corresponding author:sandeep@sameer.gov.in

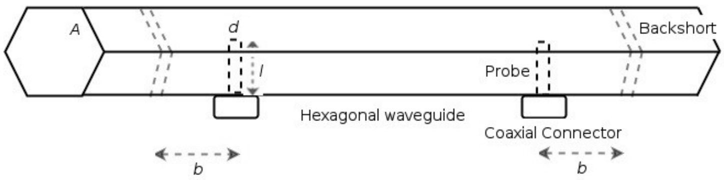

Figure 1: Geometry of the problem

2 Design and experimental setup

The geometry of the problem has been shown in Figure 1. A probe of length l and diameter d fed from a coaxial line radiates from either end inside a hexagonal waveguide having each side of length A and the radiation or reception is made unidirectional by inserting a backshorting plate at an appropriate distance b from the probe on the other side. The length l, diameter d and backshort distance b determine the matching between the coaxial feed and the waveguide. These have been optimised in this paper to design a probe for a desired band of frequencies.

2.1 Hexagonal waveguide

Hexagonal waveguides have many important applications such as polarization agile antennas and as circular polarizers, but there is little literature available on hexagonal waveguide components and their design
The hexagonal waveguide cutoff frequencies may be found to a good approximation [Zdeněk and Jiří, 2012] from the equivalent circular waveguide having the same cross sectional area as the hexagonal waveguide. This method has been used in this paper.

$$A = \frac{3\sqrt{3}}{2}a^2 = \pi r^2 \tag{1}$$

where, A is the hexagonal waveguide side length and r is the radius of equivalent circular waveguide.

2.2 Coaxial probe design

Initially, the center frequency of the band and the corresponding guide wavelength for an equivalent circular waveguide were calculated and the probe length was set equal to one fourth of the guide wavelength approximately, similar to a quarterwave monopole radiating in free space.

$$l = \frac{\lambda_g}{4} \tag{2}$$

where, λ_g is the guide wavelength and l is the length of the probe.The distance of the backshort b has also been kept equal to one fourth of the guide wavelength approximately, as this presents an open circuit at the probe and prevents unwanted radiation in the backward direction.

$$b = \frac{\lambda_g}{4} \tag{3}$$

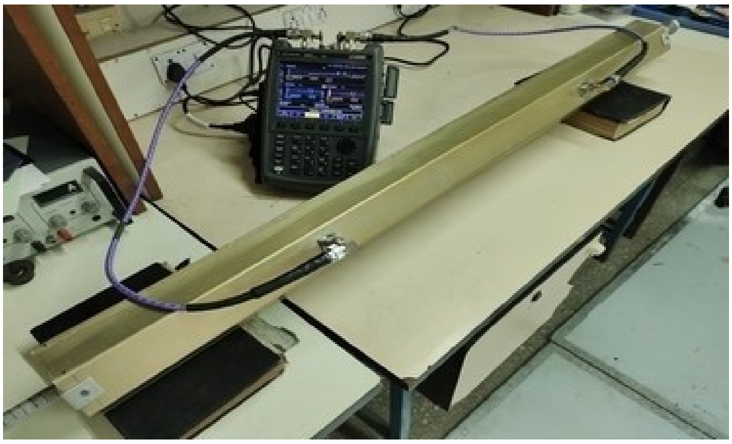

Figure 2: Fabricated hexagonal waveguide with measurement setup. The shorting plungers may be seen at either end.

The starting length of the probe and the back short for a mid-band frequency of $2.15GHz$ and bandwidth of $60MHz$ was $5.7cm$. The bandwidth has been defined here as the $2:1$ VSWR (voltage standing wave ratio) bandwidth which is often used [Rizawa and Pendleton, 1995] for defining the impedance bandwidth of microwave components and which corresponds to a return loss of $10dB$ or an acceptable power loss of 10% due to impedance mismatch. The probe length of $5.7cm$ did not give good results and the length was then further optimized by increasing it for a good match in simulation, however, the measured results showed an upward shift of approximately 2% in mid-band frequency (Table II and III). The length was further optimized taking this shift into account until a probe length of $6.9cm$ and back short distance of $8.625cm$ gave reasonably satisfactory measured results for a return loss of better than $10dB$(return loss $> 10dB$) and corresponding VSWR of better than $2:1$ (VSWR < 2).

2.3 Experimental setup

A Vector Network Analyzer (VNA) as Figure 2 was used to measure the Return loss (S11) and Transmission loss (S21) parameter, which decide the performance of the waveguide. To measure S11 and S21, initial probe length, probe diameter and shorting wall location were chosen as those given above and later on these were optimized by changing the back short length and the length of the probe until good S11 and S21 over the band were obtained.
A hexagonal waveguide of sidelength $A = 5.5cm$ corresponding to a circular waveguide with radius $r = 5cm$ having a cut-off $1.76GHz$ and a usable band up to $2.3GHz$ which is in our range of interest was fabricated by bending and brazing a chromodised Aluminum sheet of $2mm$ thickness as shown in Figure 2. A plunger with a sliding short was made and inserted at either end with an arrangement to lock it in a particular position. Measurements were taken with the arrangement shown in Figure 2 and it was noted that the measured results were in good agreement with the simulated, the mid-band frequency having been shifted up by around 2%. A few more probe lengths were simulated for better performance of the adapter and a similar good agreement between simulation and measurement was observed with the results shifted up

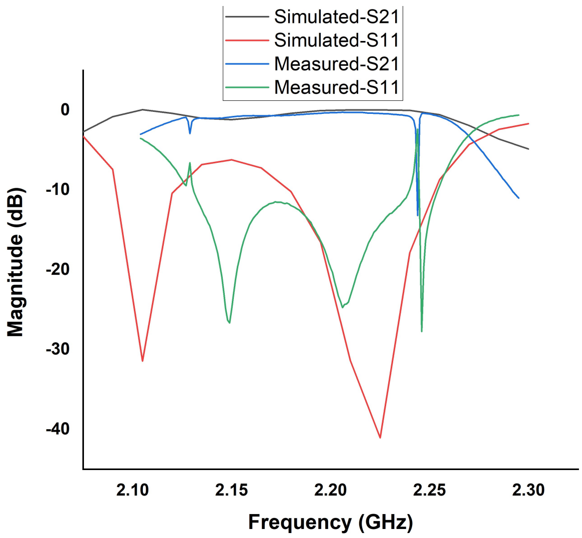

Figure 3: S11 and S21 for a probe with 8.0 cm length, 5mm diamter and 9.625 cm backshort distance.

by $1 - 2\%$. The results have been given in Section 3.

3 Simulated and measured results

The return loss (S11) and insertion loss (S21) results for the probe of $6.9cm$, $5mm$ diameter and $8.625cm$ back short length have been shown in Figure 3. The simulated results using a method of moments based software show that the waveguide is matched with a return loss better than $10dB$ over almost the entire band fro m$2.09GHz$ to $2.25GHz$ and produces a small band of frequencies where the return loss becomes just worse than $10dB$. But it was noted that the measured results have a return loss consistently better than $10dB$ over the band of $2.13 - 2.23GHz$ with a mid-band frequency of $2.18GHz$ and a bandwidth of around $100MHz$ that includes $2.15GHz$. The simulated and measured results showed a similar trend with two valleys and one hump in between which has been shown in the Figure 3. The two nulls in S11 curves in Figure 3 indicate that the waveguide presents a matched impedance to the coaxial input at these two frequencies for the given combination of probe length and back short length.

After optimization with a probe length of $8.0cm$ length, $5mm$ diameter and $9.625cm$ back short distance, the simulated waveguide, as shown in Fig.4, is matched over a $2:1$ VSWR band ($10dB$ return loss) with a mid-band frequency of $2.15GHz$ and a bandwidth of $95MHz(4.4\%)$, while in the measurement it is at $2.184GHz$ with a band of $85MHz(3.8\%)$. The shift in mid-band frequency was observed to be 1.5% on the higher side as compared with the simulated results. The two valleys in this case almost coincide with each other in frequency, although differing magnitude as seen from Figure 4.

Another simulation for a mid-band frequency around $2.145GHz$ yielded a probe length of

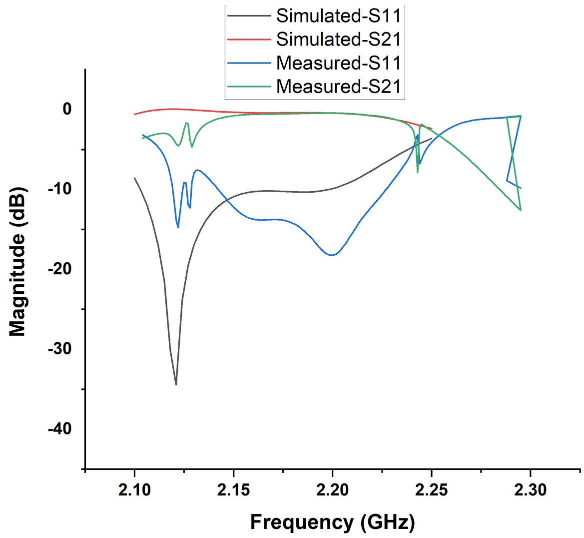

Figure 4: S11 and S21 for a probe with 8.3 cm length, 5 mm diameter and 8.625 cm backshort distance.

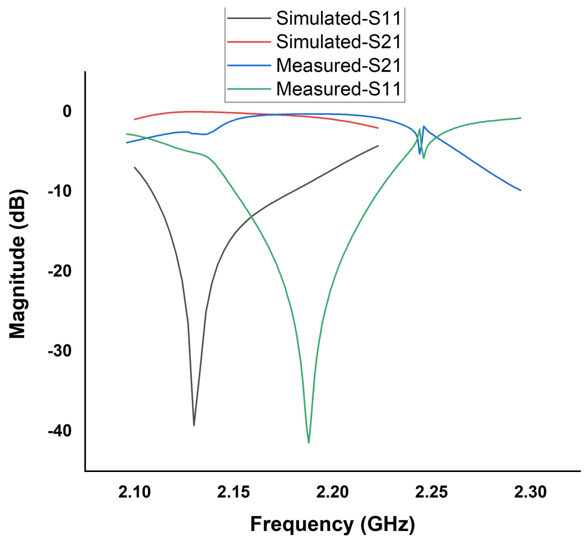

Figure 5: S11 and S21 for a probe with 8.3 cm length, 5 mm diameter and 8.625 cm backshort distance.

Table 1: Simulated and Measured Results for Probe Length $l = 6.9cm$, diameter $d = 5mm$ and Backshort distance $b = 8.625cm$

Parameter	Simulated	Measured
Midband frequency	$2.17GHz$	$2.18GHz$
Bandwidth	$160MHz$	$100MHz$
Transmission loss	Better than $1.8dB(< 1.8dB)$	Better than $1.1dB(< 1.1dB)$
Return Loss	Better than $7.5dB(> 7.5dB)$	Better than $10dB(> 10dB)$

Table 2: Simulated and Measured Results for Probe Length $l = 8.0cm$, diameter $d = 5mm$ and Backshort distance $b = 9.625cm$

Parameter	Simulated	Measured
Midband frequency	$2.15GHz$	$2.184GHz$
Bandwidth	$95MHz$	$85MHz$
Transmission loss	Better than $1dB$	Better than $1.15dB$
Return Loss	Better than $10dB$	Better than $10dB$

$8.3cm$ length, $5mm$ diameter and $8.625cm$ back short length. The simulated waveguide, as shown in Figure 5, is matched at a mid-band frequency of $2.143GHz$ with a $2:1$ VSWR band of $70MHz(3.2\%)$, while in the measurement it is at $2.194GHz$ with a band of $85MHz(3.8\%)$. The shift in frequency was observed to be 2.3% on the higher side as compared with the simulated results. A single valley is observed in this case in both simulation as well as measurements. All the results have been tabulated in Tables 1, 2 and 3.

The minor deviations in the mid-band frequency and return loss, transmission loss are because of the fabrication tolerances, small variations in the cross-section over the long waveguide, deformation due to brazing and the small gap around the periphery of the sliding short needed for the ease of sliding the back short smoothly. Within these limits, the experimental and simulated results may be seen to match with an error of about $1 - 2\%$ in mid-band frequency. Also, the probe length for any other frequency may be estimated by optimising it about 2% on the lower side in frequency to compensate for the upward shift in frequency after fabrication.

Table 3: Simulated and Measured Results for Probe Length $l = 8.3cm$, diameter $d = 5mm$ and Backshort distance $b = 8.625cm$

Parameter	Simulated	Measured
Midband frequency	$2.143GHz$	$2.194GHz$
Bandwidth	$70MHz$	$85MHz$
Transmission loss	Better than $1dB$	Better than $1.1dB$
Return Loss	Better than $10dB$	Better than $10dB$

4 Conclusion

In this paper the design and measured results of coaxial to hexagonal waveguide adapters have been presented. Three coaxial to hexagonal waveguide adapters have been simulated, fabricated and measured. It has been seen that a good match exists between the simulated and measured results and the shift in mid-band frequency for a 2 : 1 VSWR bandwidth is not more than 2.5% in the cases examined. Thus, a probe for any other frequency may be designed by optimizing it in simulation at a frequency that is about 2% lower than the operating frequency. Further optimization of probe length, diameter and shorting wall location can be done to maximize the bandwidth or to design an adapter for other bands.

Acknowledgement

The authors are thankful to all the staff of AMS Division and GFD section, SAMEER Mumbai for their help and support during the fabrication and measurement work of this activity.

References

Bhardwaj, S. and Volakis, J. (2018). Hexagonal waveguides: New class of waveguides for mm-wave circulaly polarized horns. In *2018 International Applied Computational Electromagnetics Society Symposium (ACES)*, pages 1–2. IEEE.

Bhattacharya, J. and Maity, S. (2021). Analysis of hexagonal waveguide using conformal mapping technique for dominant te mode. In *2021 2nd International Conference on Range Technology (ICORT)*, pages 1–4. IEEE.

Chen, Y. and Vaughan, R. G. (2019). Horizontally polarized array on a mast-like form for azimuthal beam switching. In *2019 IEEE 90th Vehicular Technology Conference (VTC2019-Fall)*, pages 1–5. IEEE.

Fang, Y., Lu, Z., and Yan, X. (2019). Design of an open-ended waveguide array with a plane radome. In *2019 International Conference on Microwave and Millimeter Wave Technology (ICMMT)*, pages 1–3. IEEE.

Holzman, E. L. (2005). A simple circular-to-rectangular waveguide transition. *IEEE microwave and wireless components letters*, 15(1):25–26.

Rizawa, T. and Pendleton, R. (1995). Broadband coax-waveguide transitions. In *Proceedings Particle Accelerator Conference*, volume 3, pages 1824–1826. IEEE.

Vaish, A. and Parthasarathy, H. (2010). Cutoff frequencies of electromagnetic waves propagating in a hexagonal waveguide. *International journal of microwave and optical technology*, 5(5).

Zdeněk, K. and Jiří, S. (2012). Numerical computation of cutoff frequency of irregular hexagonal waveguide. In *2012 International Conference on Applied Electronics*, pages 163–166. IEEE.